

Warming influenced by the ratio of black carbon to sulphate and the black-carbon source

M. V. Ramana¹, V. Ramanathan^{1*}, Y. Feng¹, S-C. Yoon², S-W. Kim², G. R. Carmichael³ and J. J. Schauer⁴

Black carbon is generated by fossil-fuel combustion and biomass burning. Black-carbon aerosols absorb solar radiation, and are probably a major source of global warming^{1,2}. However, the extent of black-carbon-induced warming is dependent on the concentration of sulphate and organic aerosols—which reflect solar radiation and cool the surface—and the origin of the black carbon^{3,4}. Here we examined the impact of black-carbon-to-sulphate ratios on net warming in China, using surface and aircraft measurements of aerosol plumes from Beijing, Shanghai and the Yellow Sea. The Beijing plumes had the highest ratio of black carbon to sulphate, and exerted a strong positive influence on the net warming. Compiling all the data, we show that solar-absorption efficiency was positively correlated with the ratio of black carbon to sulphate. Furthermore, we show that fossil-fuel-dominated black-carbon plumes were approximately 100% more efficient warming agents than biomass-burning-dominated plumes. We suggest that climate-change-mitigation policies should aim at reducing fossil-fuel black-carbon emissions, together with the atmospheric ratio of black carbon to sulphate.

Modelling studies have estimated that (1) the net radiative effect of black carbon (BC) and organics generated by fossil-fuel combustion and biomass-fuel cooking contribute to a warming, (2) open burning leads to net cooling^{4,5} and (3) the net warming effect of fossil-fuel BC is larger than that of biomass-fuel cooking^{6,7}. Furthermore, BC warming is regulated by the ambient concentration of sulphates resulting from sulphur dioxide (SO₂) emissions². Sulphate strongly reflects solar radiation, whereas BC strongly absorbs solar radiation. Thus the net radiative forcing is determined by the relative amounts of BC and sulphate. However, BC is invariably internally mixed with sulphates⁸ and solar absorption by BC is amplified when it is internally mixed with sulphates^{1,9,10}. Such mixtures of absorbing and scattering aerosols (including other particulate matter such as nitrate, potassium and so on) are referred to as ABCs, for atmospheric brown clouds¹¹. The Cheju ABC Plume–Monsoon Experiment (CAPMEX) conducted by us during summer 2008 provided observations for determining the dependence of the warming (or cooling) effect of ABCs on the sources of BC, and on the BC-to-sulphate ratios. The campaign was in part motivated by the mitigation of pollution from Beijing and surrounding areas during the 2008 summer Olympics¹².

CAPMEX deployed ground-level and unmanned aerial vehicle (UAV) measurements¹³ over the Yellow Sea, directly downwind of eastern China. In addition, we collected filter-based samples of aerosols during the spring of 2007 from the same location (Methods section). CAPMEX, as well as the spring 2007 samples, intercepted

aerosol plumes from Beijing, Shanghai and other East Asia regions. These plumes were classified into three categories on the basis of backward and forward trajectory analysis (Supplementary Fig. S1): (1) Beijing plumes, (2) Shanghai plumes and (3) all-others plumes, which consisted of marine sources and plumes from other East Asia regions.

Frequency distributions of the BC-to-sulphate mass-concentration ratio of surface-air samples for the three plume categories are shown in Fig. 1 (Supplementary Fig. S2). The BC mass concentrations during CAPMEX were typically in the range of 30–500 ng m⁻³, with higher BCs (>200 ng m⁻³) for continental air masses (Supplementary Fig. S2). The BC-to-sulphate ratio varied from 0 to 0.12. The highest ratios (0.04–0.12) were observed for the Beijing plumes. The mean BC-to-sulphate ratios for the Beijing, Shanghai and ‘all-others’ plumes were 0.06 ± 0.02, 0.02 ± 0.01 and 0.03 ± 0.02, respectively. Unless otherwise mentioned, uncertainties and ranges are for 95% confidence intervals. A two-tailed Student *t*-test (Supplementary Table S1) showed that the higher BC-to-sulphate ratio for the Beijing plumes was statistically significant. The higher ratio for the Beijing plume is also consistent with the large BC-to-SO₂ emission ratio¹⁴ of 0.06 for Beijing (0.02 for Shanghai; Supplementary Fig. S3). The differences in the BC-to-sulphate ratios (Fig. 1) are also reflected in the observed aerosol solar-absorption efficiency α , at 550 nm, where $\alpha = k/(k + s)$ with *k* and *s* the absorption and the scattering coefficient, respectively (see Methods section). The α values for the Beijing and Shanghai plumes are 0.1 and 0.04, respectively.

The UAV-measured vertical profiles of BC for the Beijing plume (28 Aug.) and for a plume of marine origin (31 Aug.) are shown in Fig. 2a, along with the mean profiles for the Beijing plumes (4 days) and the Marine plumes (4 days). Data from 28 and 31 Aug. were chosen because these were the only two clear-sky (cloudless) days available, and clear-sky data yield the most reliable solar-heating rates. With the arrival of the Beijing plume, BC concentrations at 0.75 km altitude increased from 85 ng m⁻³ to more than 500 ng m⁻³, and at 3.0 km increased from near zero to 250 ng m⁻³. The BC vertical profiles for the Marine plume (31 Aug.) and the Beijing plume (28 Aug.) are very similar (within instrumental uncertainties) to their respective 4 day average profiles, which suggests that the profiles for the two dates are typical of the Marine and the Beijing plumes for this period. This similarity is important for the interpretation of the measured heating rates because UAV heating rates are available for only 28 and 31 Aug.

The broadband (0.3–2.8 μm) diurnal mean solar heating rates, *H*, (Fig. 2b) at 3 km altitude for the Marine and the Beijing plume conditions are 0.77(±0.07) and 1.01(±0.08) K d⁻¹, respectively,

¹Scripps Institution of Oceanography, UCSD, 9500 Gilman Drive, La Jolla, California 92093, USA, ²School of Earth and Environmental Sciences, Seoul National University, Seoul 151-747, South Korea, ³College of Engineering, University of Iowa, Iowa City, Iowa 52240, USA, ⁴Environmental Chemistry and Technology Program, University of Wisconsin–Madison, Madison, Wisconsin 53706, USA. *e-mail: vramanathan@ucsd.edu.

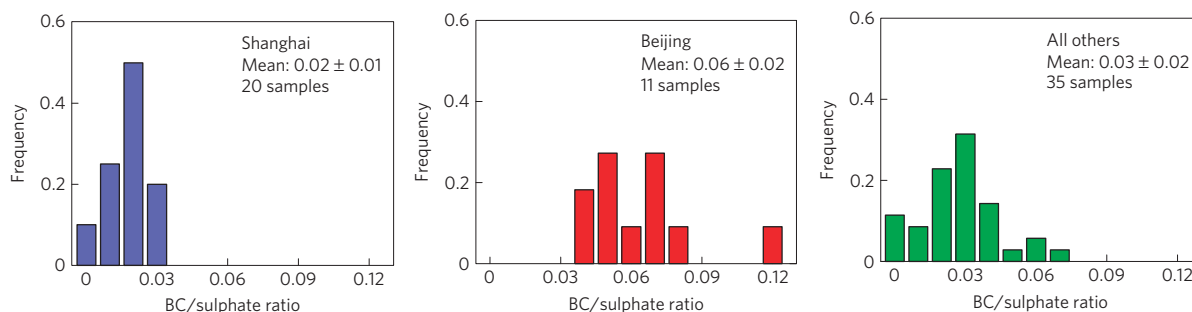


Figure 1 | Frequency distribution of the BC-to-sulphate mass-concentration ratio for the Shanghai plumes, the Beijing plumes and the 'all-others' plumes measured at the Gosan climate observatory. The data include 2007 spring data along with the CAPMEX data. The mean value for each plume category is shown in the figure along with the 95% confidence intervals. Uncertainties in the measurements are given in the Methods section.

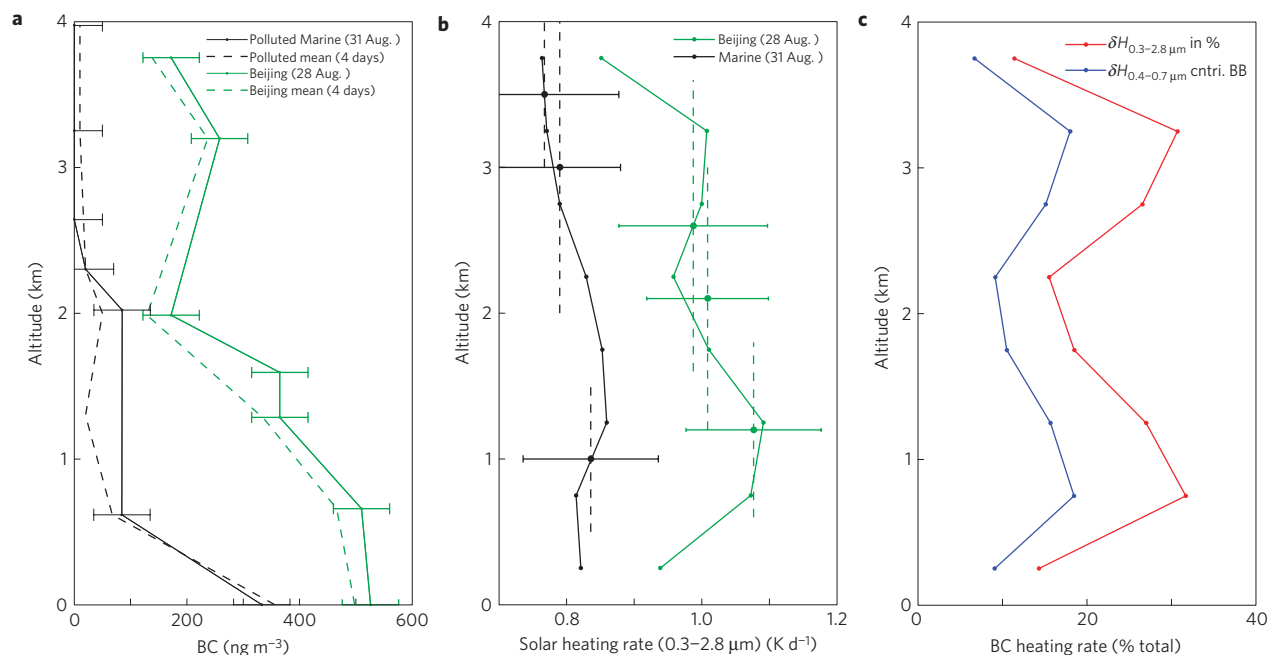


Figure 2 | Vertical profiles determined from the UAV data. a, BC concentration profiles for the Marine plumes and the Beijing plumes. **b,** Broadband (0.3–2.8 μm) diurnal averaged solar-heating rate (H) profiles for the Marine and the Beijing plumes. The vertical dashed lines indicate the layer depths, the thick solid circles are the observed values and the continuous lines are the values simulated by the Monte Carlo Aerosol Cloud Radiation model. The horizontal bars in **a** and **b** indicate the uncertainties in the measurements (see Methods section). **c,** The percentage contribution by BC to H ($\delta H_{0.3-2.8 \mu\text{m}}$ in %) and the percentage contribution by solar absorption in the visible range (0.4–0.7 μm) to H ($\delta H_{0.4-0.7 \mu\text{m}}$ cntri. BB).

whereas the H values within the mixed layer (~ 0.75 km) are $0.81(\pm 0.08)$ and $1.07(\pm 0.1)$ K d^{-1} , respectively. The enhancements in H between the two periods (δH) at 0.75 km and 3 km altitudes are about $0.26(\pm 0.13)$ K d^{-1} and $0.24(\pm 0.11)$ K d^{-1} , respectively. The visible solar absorption accounts for roughly half of the increase in the broadband solar heating (Fig. 2c; Supplementary Fig. S4), which confirms that the enhancement is due to BC. Another confirmation for the large enhancement of heating by BC is provided by the H for the South Asia plume^{13,15} (Supplementary Table S2), also determined with UAVs over the Northern Indian Ocean. For the 0.5–3 km layer, the South Asia data revealed an increase of solar heating of $0.6(\pm 0.15) \times 10^{-3}$ K d^{-1} per ($\mu\text{g m}^{-2}$) of BC, which is very similar to the Beijing-plume BC heating value of $0.5(\pm 0.2) \times 10^{-3}$ K d^{-1} per ($\mu\text{g m}^{-2}$). The close agreement validates the reliability and the statistical significance of the inferred BC heating rates.

The measured BC-to-sulphate mass-concentration ratios are plotted as a function of α in Fig. 3 for the South¹¹ and the East Asia plumes. Theoretically, α can vary between zero (totally

reflecting aerosol) and one (totally absorbing aerosol). The presence of BC and other anthropogenic aerosols over the Arabian Sea observatory varies with the seasonal Indian Monsoon¹¹. From June to September the wet monsoon brings marine air into the region and the BC-to-sulphate ratio and α values are close to zero, with occasional occurrences of higher α values (about 0.05). Commercial shipping is an important source of BC in the marine environment and the emitted aerosols usually have low BC-to-sulphate ratios owing to the use of low-quality unregulated fuels that are high in sulphur¹⁶. Accordingly, the wet-season BC data are labelled as 'Ship BC'. Conversely, the dry monsoon brings polluted air from the Indian subcontinent and Southeast Asia during November through April. As a result, high BC-to-sulphate ratios (up to 0.16) and high α values (up to 0.1) are observed during the dry season.

For all three cases shown in Fig. 3 (East Asia, South Asia and 'ship BC'), α values increased significantly with the BC-to-sulphate ratio. However, the slope of the increase depends strongly on the source region (Supplementary Table S3). The slope of $1.17(\pm 0.28)$ for the East Asia aerosols is a factor of 2.5 larger than that of the South Asia

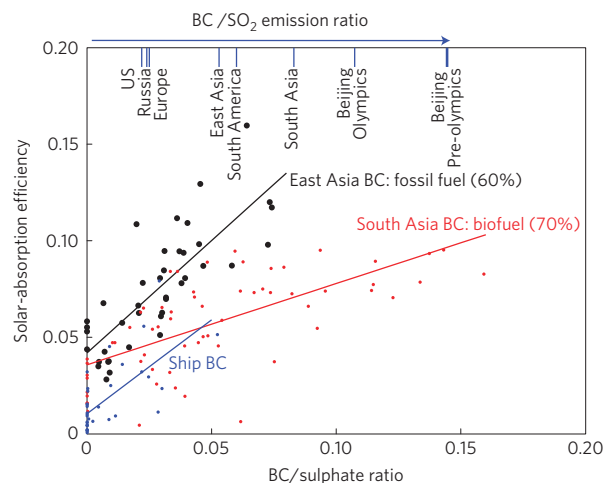


Figure 3 | Measured BC-to-sulphate mass-concentration ratio versus aerosol solar-absorption efficiency, that is, α , at 550 nm. The black data points represent East Asia data collected during CAPMEX, whereas the red and the blue points represent South Asia data during the dry- and the wet-monsoon ('Ship BC') seasons, respectively. The continuous lines are the best-fit lines (Supplementary Table S3). The top section in the figure indicates the regional and the annual mean BC-to-SO₂ emission ratios for different regions²⁹. The BC-to-SO₂ emission ratios for Beijing before and during the Olympics¹² are also shown.

aerosols [0.42(±0.13)]. The correlation coefficients range from 0.7 to 0.8. The largest α values were observed for the East Asia aerosols, with the Beijing plume having the highest values. For the same BC-to-sulphate ratio, α values for the East Asia aerosols are about a factor of two larger than those for the South Asia aerosols. One main difference between the East Asia and the South Asia aerosols is the relative contribution by fossil fuel and biomass fuel to BC emissions. The fossil-fuel contribution to the total BC is about 60% over East Asia and is only about 30% over South Asia on the basis of emission inventories¹⁶. The results suggest that the absorption efficiency is larger in fossil-fuel-based plumes, but these inventories are subject to large uncertainties^{14,16}. However, observation-based atmospheric-aerosol source-apportionment studies also show that fossil-fuel combustion is the main source for BC in East Asia¹⁴, whereas biomass-fuel BC is the main source in South Asia^{8,17}. Although such source-apportionment studies are also subject to uncertainties, they are significantly more constrained than emission inventories^{18,19}. Another result that supports the larger absorption efficiency of fossil-fuel plumes containing BC is that the slope for the ship BC (0.97 ± 0.38) is similar to the East Asia aerosol slope (1.17 ± 0.28) (Fig. 3). The inference is that, for the same BC-to-sulphate ratio, α is much larger for fossil-fuel-based plumes. This supports the model-derived conclusion^{3,4} that fossil-fuel BC is more effective as a warming agent compared with BC from biomass fuels. As data from East Asia are for one season, whereas the South Asia data include all seasons of a year, we conducted another consistency test. We plotted the measured absorption coefficient (as opposed to α) as a function of the BC concentrations (Supplementary Fig. S5), and the slope for the single-season data of the East Asia aerosols was nearly identical to that of the South Asia data. Likewise, agreement for the UAV-measured BC heating for the two regions (discussed earlier), in spite of the differences in the season and year of data collection, reveals an overall consistency in the present approach for elucidating the source dependence of the aerosol warming. These findings have significant implications for the role of BC in twentieth-century temperature trends, which are explored next.

The ratio of fossil-fuel-based black carbon, BC_{ff}, to SO₂ emissions^{20–22} has increased by more than a factor of two during

the twentieth century, and the ratio of BC_{ff} to BC_{Total} (that is, Total = fossil + biomass fuels BC) has also increased threefold (Supplementary Fig. S6). Using the slopes and offsets in Fig. 3, we infer that the increase in these two ratios should have contributed about 0.11 W m⁻² to the global radiative forcing, which is 12–30% of the global BC forcing of 0.35 W m⁻² (ref. 4)–0.9 W m⁻² (ref. 2) (Supplementary Table S4). Equally important is the 0.56 W m⁻² increase in the global mean atmospheric heating (Supplementary Table S4), which has implications for the Asian monsoon^{2,23} and the warming trends over the elevated regions of Tibet and the Himalayas^{13,24}. The largest BC_{ff}/BC_{Total} values now are found in Europe, USA and East Asia. Asia is also subject to large ratios of BC-to-SO₂ emissions ranging from 0.05 to 0.15 (Fig. 3). The ratio over Beijing is about 0.12 during the summer. It is encouraging to note that the emission controls implemented in 2008 were successful in reducing Beijing emissions of BC (ref. 12) by about 25%, as well as reducing the ratio of BC to SO₂ by about 20%. Because of its short lifetime, BC offers the greatest potential for slowing down climate change in the coming decades. Worldwide there are efforts to decrease SO₂ emissions, and the data presented in this study strongly suggest that such reductions should be accompanied by larger percentage reductions in BC, such that the BC-to-SO₂ emission ratio is also decreased. Such a mitigation step will also have significant co-benefits to human health, because air pollution leads to over two million deaths annually²⁵.

Methods

Measurements. The unmanned-aircraft-measurement component of the CAPMEX took place during Aug.–Sept. 2008 in three phases. Phase 1 (9–25 Aug.) was launched from Jeongseok Airport (33° 23' N, 126° 42' E, 1,950 m above mean sea level); Phase 2 (27 Aug.–11 Sept.) and Phase 3 (16–30 Sept.) were launched from Sangmo-ri Airfield (33° 12' N, 126° 16' E). Sangmo-ri Airfield is on the southwestern tip of Cheju and is ~10 miles away from Gosan Climate Observatory (GCO). A suite of aerosol, cloud and radiation instruments that were flown during the Maldives Autonomous Unmanned Aerial Vehicle Campaign¹³ was deployed during the CAPMEX campaign. The details of the uncertainties in aerosol²⁶ and radiation¹⁵ instruments are given in previous papers. In general, the science missions consisted of stacked missions involving two UAVs designed to capture measurements of atmospheric heating rates and aerosol-cloud radiation, and single-platform missions for vertical profiling.

Another important component of the CAPMEX measurement programme was the surface measurements carried out at the GCO from July to Sept. 2008. This observatory is one of the supersites of the Project Atmospheric Brown Clouds¹¹. The GCO (33° 17' 32" N, 126° 09' 42" E, 50 m above mean sea level) is located on the western tip of Cheju Island facing the Yellow Sea and has housed several previous field campaigns^{11,27}. The GCO contains a suite of aerosol, gaseous, radiation and cloud microphysics instruments, including a lidar and balloon-sondes for vertical distribution of particles and meteorological parameters, respectively. Moreover, filter sampling at GCO provided 24-h-integrated direct measurements of elemental/black-carbon mass, organic-carbon mass, total-aerosol mass, inorganic ions and tracers. The filters were analysed by a thermal optical method²⁷. Elemental carbon is obtained from chemical measurements, whereas BC is an optical measurement and hence may include absorption due to organics, or so-called brown carbon²⁸. The uncertainty in BC mass concentration is ±0.075 μg m⁻³ and the uncertainty in sulphate mass concentration is ~±3.5%. The filter-sampling data collected at GCO during spring 2007 were also included in the present data analysis.

The solar-absorption efficiency, α , is related to the single-scattering albedo (SSA) through the equation $\alpha = 1 - \text{SSA}$. The diurnal mean solar-heating rates (H) were estimated from the observed upward and downward solar fluxes measured from the UAVs (Fig. 2b), following the procedures in ref. 15. The diurnal mean solar-flux values were calculated by using the daytime measured fluxes at each altitude fitted to an estimated diurnal flux curve produced with the Monte Carlo Aerosol Cloud Radiation model^{13,15}.

Received 15 February 2010; accepted 22 June 2010;
published online 25 July 2010

References

- Jacobson, M. Z. Strong radiative heating due to the mixing state of black carbon in atmospheric aerosols. *Nature* **409**, 695–697 (2001).
- Ramanathan, V. & Carmichael, G. Global and regional climate changes due to black carbon. *Nature Geosci.* **1**, 221–227 (2008).

3. Jacobson, M. Z. Control of fossil-fuel particulate black carbon and organic matter, possibly the most effective method of slowing global warming. *J. Geophys. Res.* **107**, 4410 (2002).
4. Forster, P. *et al.* in *Climate Change 2007: The Physical Science Basis—Contribution of Working Group I to the Fourth Assessment Report of the Intergovernmental Panel on Climate Change* (eds Solomon, S. *et al.*) (Cambridge Univ. Press, 2007).
5. Jacobson, M. Z. The short-term cooling but long-term global warming due to biomass burning. *J. Clim.* **17**, 2909–2926 (2004).
6. Jacobson, M. Z. Climate response of fossil fuel and biofuel soot, accounting for soot's feedback to snow and sea ice albedo and emissivity. *J. Geophys. Res.* **109**, D21201 (2004).
7. Bond, T. C. Can warming particles enter global climate discussions? *Environ. Res. Lett.* **2**, 045030 (2007).
8. Guazzotti, S. A., Coffee, K. R. & Prather, K. A. Continuous measurements of size-resolved particle chemistry during INDOEX-Intensive Field Phase 99. *J. Geophys. Res.* **106**, 28607–28628 (2001).
9. Moffet, R. C. & Prather, K. A. *In-situ* measurements of the mixing state and optical properties of soot with implications for radiative forcing estimates. *Proc. Natl Acad. Sci.* **106**, 11872–11877 (2009).
10. Novakov, T. *et al.* Origin of carbonaceous aerosols over the tropical Indian Ocean: Biomass burning or fossil fuels? *Geophys. Res. Lett.* **27**, 695–697 (2001).
11. Ramanathan, V. *et al.* Atmospheric brown clouds: Hemispherical and regional variations in long range transport, absorption, and radiative forcing. *J. Geophys. Res.* **112**, D22S21 (2007).
12. United Nations Environment Programme Independent Environmental Assessment: Beijing 2008 Olympic Games. (UNEP, 2009). Data are available at <http://mic.greenresource.cn/olympic>; Emission inventory prepared by Argonne National Laboratory and Tsinghua University.
13. Ramanathan, V. *et al.* Warming trends in Asia amplified by brown cloud solar absorption. *Nature* **448**, 575–578 (2007).
14. Zhang, Q. *et al.* Asian emissions in 2006 for the NASA INTEX-B mission. *Atmos. Chem. Phys.* **9**, 5131–5153 (2009).
15. Ramana, M. V., Ramanathan, V., Kim, D., Roberts, G. C. & Corrigan, C. E. Albedo, atmospheric solar absorption and heating rate measurements with stacked UAVs. *Q. J. R. Meteorol. Soc.* **133**, 1913–1931 (2007).
16. Bond, T. C. *et al.* A technology-based global inventory of black and organic carbon emissions from combustion. *J. Geophys. Res.* **109**, D14203 (2004).
17. Gustafsson, O. *et al.* Brown clouds over South Asia: Biomass or fossil fuel combustion? *Science* **323**, 495–498 (2009).
18. Sheesley, R. J., Schauer, J. J., Zheng, M. & Wang, B. Sensitivity of molecular marker-based CMB models to biomass burning source profiles. *Atmos. Environ.* **41**, 9050–9063 (2007).
19. Lough, G. C. & Schauer, J. J. Sensitivity of source apportionment of urban particulate matter to uncertainty in motor vehicle emission profiles. *J. Air Waste Manage. Assoc.* **57**, 1200–1213 (2007).
20. Ito, A. & Penner, J. E. Historical emissions of carbonaceous aerosols from biomass and fossil fuel burning for the period 1870–2000. *Glob. Biochem. Cycles* **19**, GB2028 (2005).
21. Olivier, J. G. J., Van Aardenne, J. A., Dentener, F., Ganzeveld, L. & Peters, J. A. H. W. in *Non-CO₂ Greenhouse Gases (NCGG-4)* (ed. van Amstel, A. (coord.)) 325–330 (Mill Press, 2005).
22. Smith, S. J., Andres, R., Conception, E. & Lurz, J. *Historical Sulfur Dioxide Emissions 1850–2000: Methods and Results, JGCRI Report*. PNNL-14537 (Pacific Northwest National Laboratory, 2004).
23. Menon, S. *et al.* Black carbon aerosols and the third polar ice cap. *Atmos. Chem. Phys. Discuss.* **9**, 26593–26625 (2009).
24. Lau, K.-M. *et al.* The Joint Aerosol–Monsoon Experiment: A new challenge for monsoon climate research. *Bull. Am. Meteorol. Soc.* **89**, 1–5 (2008).
25. Smith, K. R. In praise of petroleum, editorial. *Science* **298**, 1847 (2002).
26. Corrigan, C. E., Roberts, G. C., Ramana, M. V., Kim, D. & Ramanathan, V. Capturing vertical profiles of aerosols and black carbon over the Indian Ocean using autonomous unmanned aerial vehicles. *Atmos. Chem. Phys.* **8**, 737–747 (2008).
27. Schauer, J. J. *et al.* ACE–Asia intercomparison of a thermal-optical method for the determination of particle-phase organic and elemental carbon. *Environ. Sci. Technol.* **37**, 993–1001 (2003).
28. Andreae, M. O. & Gelencser, A. Black carbon or brown carbon? The nature of light-absorbing carbonaceous aerosols. *Atmos. Chem. Phys.* **6**, 3131–3148 (2006).
29. Streets, D. G. *et al.* Anthropogenic and natural contributions to regional trends in aerosol optical depth, 1980–2006. *J. Geophys. Res.* **114**, D00D18 (2009).

Acknowledgements

The CAPMEX campaign was supported by NSF under grant ATM-0836093, and the analyses were funded by NSF grant ATM-0721142 and by NOAA grant NOAA/NA17RJ1231. We thank H. Nguyen for his support and the flight crew from Advanced Ceramic Research for the field support. We are grateful to Korean Air and their staff at Jeongseok Airport for their generous hospitality. S.-C.Y. was supported by the Korean Meteorological Administration R&D programmes under grant CATER 2006-4104, and the BK21 program in the School of Earth and Environmental Sciences, Seoul National University. We thank J. Fein, M. Rezin, S. C. Park, M. H. Kim, E. A. Stone and J. DeMinter for their support in conducting the campaign. We would like to acknowledge Cheju Aviation Management Office for their support of the field campaign.

Author contributions

M.V.R. collected the data and carried out the bulk of the analysis with major input from V.R., V.R. designed CAPMEX and provided project oversight, Y.F. was responsible for emission-data analysis, Gosan surface data were synthesized by S.-C.Y. and S.-W.K., G.R.C. was responsible for the emission data during the Olympics and J.J.S. was responsible for aerosol filter-sampling analysis. V.R. and M.V.R. wrote the manuscript, with input from Y.F., S.-C.Y., S.-W.K., G.R.C. and J.J.S.

Additional information

The authors declare no competing financial interests. Supplementary information accompanies this paper on www.nature.com/naturegeoscience. Reprints and permissions information is available online at <http://npg.nature.com/reprintsandpermissions>. Correspondence and requests for materials should be addressed to V.R.